Detachment of Microtubules Driven by Kinesin Motors from Track Surfaces Under External Force

May Sweet(✉) and Takahiro Nitta(✉)

Gifu University, Gifu 501-1193, Japan
x3915007@edu.gifu-u.ac.jp, nittat@gifu-u.ac.jp

Abstract. Motor proteins, such as myosin and kinesin, are biological molecular motors involved in force generation and material transport in living cells. Motor proteins and their associated cytoskeletal filaments, such as actin filaments and microtubules, have been utilized for active transport in engineered systems. In controlling the active transport, external forces via electric fields or fluid flow were commonly used. A drawback of using external force is that the external force can cause detachment of microtubules from gliding surfaces. Detachment leads to loss of cargo or sparse surface density of microtubules, thus limiting the availability of external forces. Detachment should be minimized. In doing so, detailed observation on the process of detachment would be helpful. However, due to its limited spatial and temporal resolution, experimental investigations are hampered. Here, we show a simulation study for the detachment of microtubules gliding over surfaces coated with kinesin motors by an external force. Owing to the computer simulation's high spatial and time resolution, two modes of detachment were found. Detailed processes of the two modes were revealed, which would be useful to diminish detachment.

Keywords: Biomolecular motor · Cytoskeletal filaments · Computer simulation

1 Introduction

Motor proteins, such as myosin and kinesin, are biological molecular motors working for force generation and intracellular transport. In the last two decades, they have been utilized in engineered systems [1]. Molecular shuttles driven by motor proteins are essential for active transport in such devices, where cytoskeletal filaments carrying analytes [2–4] or information [5, 6] are transported along predefined tracks covered with associated motor proteins to designated destinations.

To control the movements of molecular shuttles, external forces via electric fields or fluid flow were commonly used [7–9]. While the larger applied force leads to better control, the drawback is the detachment of molecular shuttles from surfaces over which they glide [8]. The detachments lead to loss of cargo and the sparse surface density of molecular shuttles [10], which limits device performance and should be minimized.

T. Nakano (Ed.): BICT 2021, LNICST 403, pp. 199–206, 2021.
https://doi.org/10.1007/978-3-030-92163-7_16

In addition, while trajectories without detachment can be predicted with computer simulations [11, 12], detachment makes such prediction difficult, bringing complications in designing devices. A detailed mechanism of the detachment of molecular shuttles would be helpful to their suppression. However, the process of detachment is abrupt compared to spatial and temporal limitations in experiments so that detailed mechanisms of detachment remain unknown.

Here, to investigate detailed mechanisms of the detachment of the molecular shuttles, we used our own developed computer simulation. The use of the computer simulation enables us to reveal a detailed mechanism of the detachment, which cannot be obtained in experimental investigation. In the present study, we found that there are two distinct modes of microtubule detachment: unzipping/swiveling and jumping. Owing to the high time resolution of the simulation, we observed the two detachment modes with around 1,000 times higher time resolution than that of a conventional microscope. Our observation will guide the detailed understanding of the mechanism of the detachment of molecular shuttles driven by the kinesin motor.

2 Simulation Method

The simulation method was developed based on a previous study [13] and is briefly described as follows.

Microtubules were modeled as inextensible elastic beams with a bending rigidity of 22 pN/μm^2 subjected to thermal fluctuations and applied force, represented by bead-rod polymers. The applied force acting on microtubules was represented by the force acting on the beads. The length of the microtubules was 5 μm, compatible with the length of microtubules commonly used in experiments.

Microtubules were propelled by kinesin motors, which are modeled as a linear spring with a spring constant of 100 pN/μm and with zero equilibrium length. The heads of the kinesin motors moved toward the microtubule plus end, while the tails of kinesin motors were fixed on the substrate, building up tension to move the microtubules toward their minus ends.

The equations of motion of beads consisting of microtubules were expressed to be

$$\boldsymbol{r}'_i(t+\Delta t) = \boldsymbol{r}_i(t) + \frac{\Delta t}{\zeta}\left(\boldsymbol{F}_{b,i} + \boldsymbol{F}_{k,i} + \boldsymbol{F}_{ex,i}\right) + \sqrt{2D\cdot\Delta t}\cdot\boldsymbol{\xi}_i,$$

where ζ is the viscous drag coefficient, $\boldsymbol{F}_{b,i}$ is the force due to bending of microtubules, $\boldsymbol{F}_{k,i}$ is the force exerted by kinesin motors, $\boldsymbol{F}_{ex,i}$ is an external force, $\boldsymbol{\xi}_i$ is a three-dimensional random vector whose components take random values with zero mean and standard deviation of one. The last term of the right-hand side of the equation represents the thermal fluctuation of the beads. The calculated positions, $\{\boldsymbol{r}'_i(t+\Delta t)\}$, were corrected to have an assigned distance of 0.25 μm between them.

3 Results

3.1 Trajectories Under High External Forces

Figure 1 shows representative trajectories of microtubules gliding over kinesin motors with a surface motor density of 10 μm^{-2} under an external force of 5.0 pN/μm.

The trajectories showed intermittencies reflecting partial or whole microtubule detachment from the surface. In contrast, trajectories with higher motor density and/or weaker external force did not show such intermittencies. Since the partial and whole microtubule detachments occurred stochastically, the control of microtubule movement was diminished.

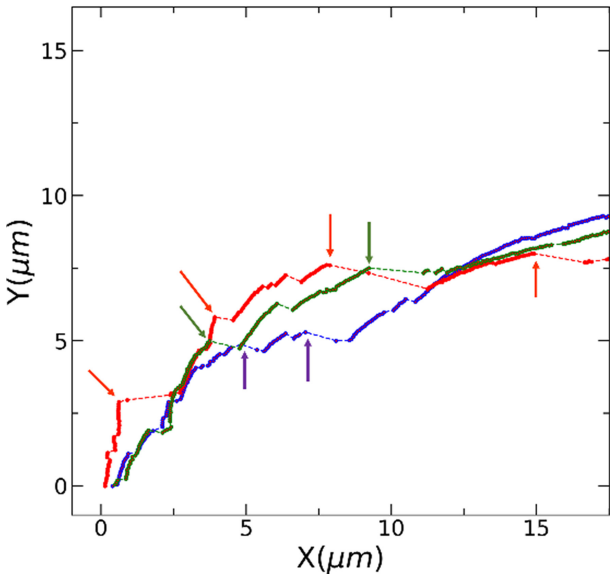

Fig. 1. Representative trajectories of microtubules gliding over kinesin motors with a surface motor density of 10 μm^{-2} under an external force of 5.0 pN/μm. Different colors represent different microtubule trajectories. Jumps are denoted with arrows. Only major jumps are marked for visibility.

To quantify the intermittencies in the trajectories, the instantaneous speed of leading tips and trailing ends were calculated (Fig. 2). Reflecting the partial and whole microtubule detachments, the time evolutions of the instantaneous speeds showed sharp isolated peaks over the average speed of 0.8 μm/s. The instantaneous speeds at the peaks could reach more than 50 times the average speed of 0.8 μm/s. The instantaneous speed showed an exponential distribution. No significant difference was observed between distributions of the leading tips and trailing ends (Fig. 3). This observation indicated that detachments equally occurred from both the leading tips and trailing ends.

We found that detachment processes can be categorized into two classes: unzipping/swiveling (Fig. 4a) and jumping (Fig. 4b). We will describe each process and mechanism in the following sections.

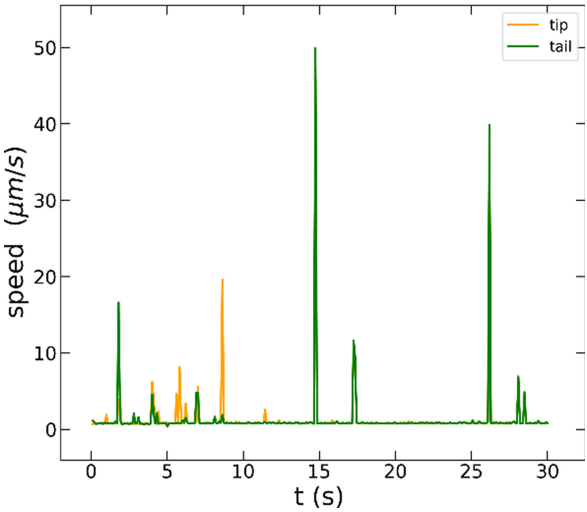

Fig. 2. Time evolutions of instantaneous speeds of the leading tip and trailing end of a microtubule.

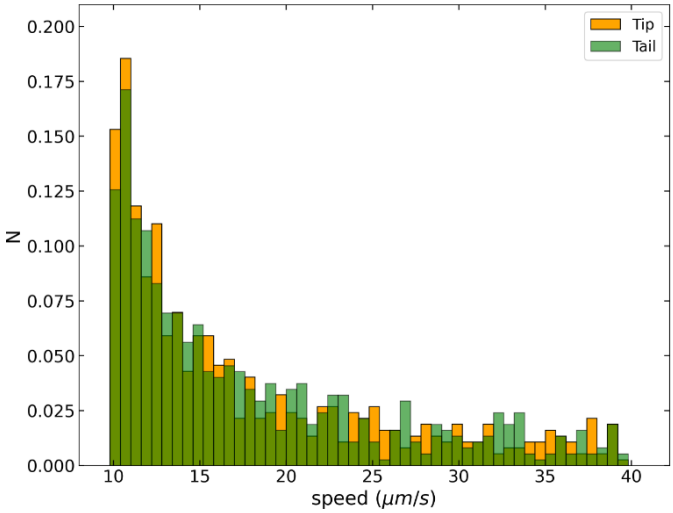

Fig. 3. Histograms of instantaneous speeds of the leading tips and trailing ends of 60 microtubules. To highlight the abrupt changes in gliding speed corresponding to the peaks in Fig. 2, only the part with the speed >1.0 μm/s is shown.

3.2 Unzipping/Swiveling of Microtubule

Unbinding of kinesin motors from microtubules successively occurred from either the leading tip or the trailing end, which we call unzipping. A representative microtubule undergoing unzipping followed by swiveling is shown in Fig. 4a observed with 0.1 s time resolution. The 0.1 s time resolution could not clearly identify the phenomenon

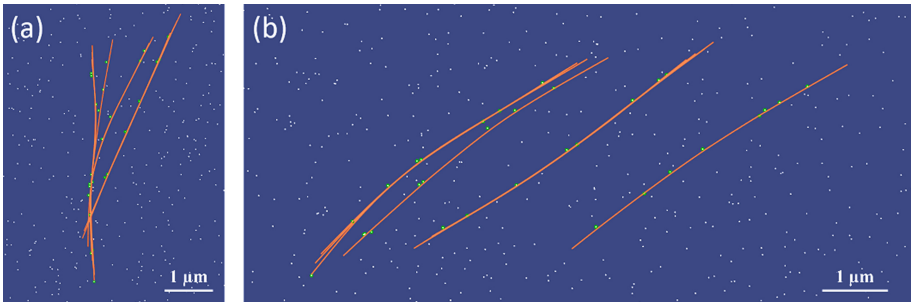

Fig. 4. Unzipping/swiveling (a) and jump (b) observed with 0.1 s time resolution. The orange lines represent superimposed conformations of a microtubule. White dots represent kinesin motors. Green dots represent kinesin motors binding to the microtubule. (Color figure online)

of microtubules detachment. To identify the detailed phenomenon of microtubules, we magnified with 1,000 times higher time resolution in Fig. 5. Part of the microtubules showed lateral shifts a few times. Upon unzipping, the population of binding kinesin motors was gradually replaced. Between the shifts, microtubules showed thermal fluctuations without changing the population of binding kinesin motors. After unzipping, swiveling of microtubules occasionally followed, which caused further changes in their gliding direction.

While unzipping was equally likely to occur from both ends, unzipping from leading tips affected trajectories more significantly than that from the trailing ends, since trajectories are mostly determined by their leading tips. Unzipping/swiveling tended to occur more often when the microtubules were moving perpendicular to an applied force.

3.3 Jump of Microtubule

In contrast to unzipping/swiveling, the jumps abruptly occurred within 0.1 s time resolution. In many cases, the positions of microtubules just shifted downstream of the applied force without significant change of direction. A representative microtubule undergoing jump is shown in Fig. 6 observed with 0.1 ms time resolution. Upon jump, the whole population of binding kinesin motors was replaced. Distance during the jump varies and can be more than the length of microtubules. The jumps observed with a 0.1 s time window consisted of smaller jumps without changing the direction of microtubules.

The jumps of microtubules were observed with almost equal frequency all the way along the trajectories. The jump of microtubules was greatly diminished by lowering the applied force from 5.0 pN/μm to 4.0 pN/μm.

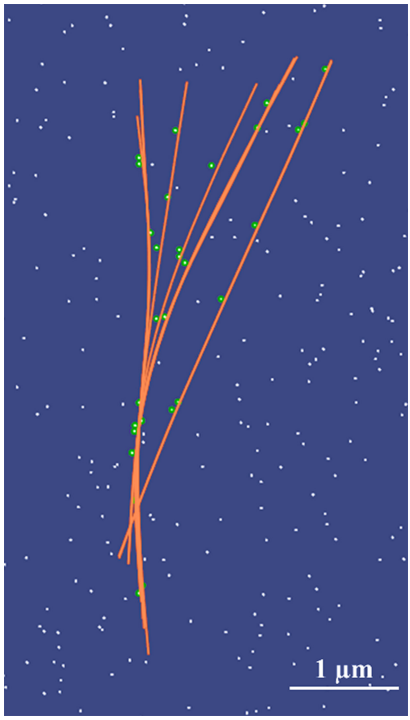

Fig. 5. Unzipping and swiveling observed with 0.1 ms time resolution. The orange lines represent superimposed conformations of a microtubule. White dots represent kinesin motors. Green dots represent kinesin motors binding to the microtubule. (Color figure online)

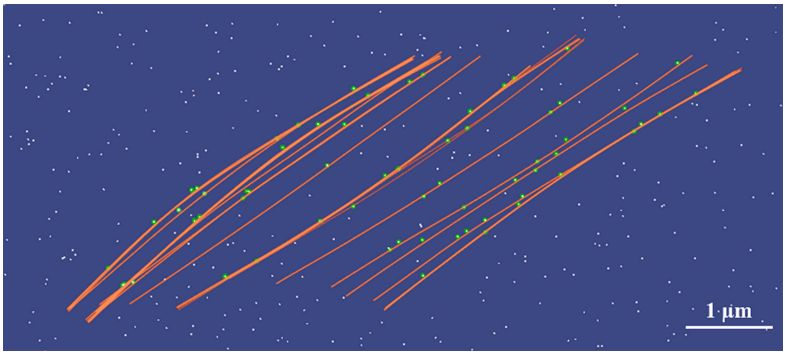

Fig. 6. A series of small jumps observed with 0.1 ms time resolution. The orange lines represent the superimposed conformations of a microtubule. White dots represent kinesin motors. Green dots represent kinesin motors binding to the microtubule. (Color figure online)

4 Discussion

By using our own developed computer simulation, we investigated the detailed mechanism of the detachment of molecular shuttles driven by kinesin motors. We found that there were two modes of detachment, unzipping/swiveling and jumping. Unzipping/swiveling can be characterized by the sequential unbinding of kinesin motors from microtubules from either the leading tips or the trailing ends. On the other hand, jumping can be characterized by sudden shifts of microtubule position toward the downstream of the external force without significant change of their direction. These kinds of observations were not obtained before because of limited space and time resolution in experiments.

Based on our observations reported here, to diminish the detachment of microtubules from track surfaces, one should take note of the following two. Firstly, the applied force should be lower than the force inducing a significant occurrence of jump of microtubules. Secondly, to avoid unzipping/swiveling of microtubules, a strong external force should not be applied when the microtubules are moving perpendicularly to the force.

References

1. Saper, G., Hess, H.: Synthetic systems powered by biological molecular motors. Chem. Rev. **120**(1), 288–309 (2020). https://doi.org/10.1021/acs.chemrev.9b00249
2. Lin, C.T., Kao, M.T., Kurabayashi, K., Meyhofer, E.: Self-contained, biomolecular motor-driven protein sorting and concentrating in an ultrasensitive microfluidic chip. Nano. Lett. **8**(4), 1041–1046 (2008). https://doi.org/10.1021/nl072742x
3. Fischer, T., Agarwal, A., Hess, H.: A smart dust biosensor powered by kinesin motors. Nat. Nanotechnol. **4**(3), 162–166 (2009). https://doi.org/10.1038/nnano.2008.393
4. Lard, M., et al.: Ultrafast molecular motor driven nanoseparation and biosensing. Biosens. Bioelectron. **48**, 145–152 (2013). https://doi.org/10.1016/j.bios.2013.03.071
5. Nakano, T., Moore, M.J., Wei, F., Vasilakos, A.V., Shuai, J.: Molecular communication and networking: opportunities and challenges. IEEE Trans. Nanobioscience **11**(2), 135–148 (2012). https://doi.org/10.1109/TNB.2012.2191570
6. Farsad, N., Yilmaz, H.B., Eckford, A., Chae, C.B., Guo, W.: A comprehensive survey of recent advancements in molecular communication. IEEE Commun. Surv. Tutorials **18**(3), 1887–1919 (2016). https://doi.org/10.1109/COMST.2016.2527741
7. Van Den Heuvel, M.G.L., De Graaff, M.P., Dekker, C.: Molecular sorting by electrical steering of microtubules in kinesin-coated channels. Science **312**(5775), 910–914 (2006). https://doi.org/10.1126/science.1124258
8. Agayan, R.R., et al.: Optimization of isopolar microtubule arrays. Langmuir **29**(7), 2265–2272 (2013). https://doi.org/10.1021/la303792v
9. Isozaki, N., Shintaku, H.,Kotera, H., Hawkins, T.L., Ross, J. L., Yokokawa, R.: M I C R O R O B O T S Control of molecular shuttles by designing electrical and mechanical properties of microtubules. [Online]. Available http://robotics.sciencemag.org/ (2017)
10. Bassir Kazeruni, N.M., Rodriguez, J.B., Saper, G., Hess, H.: Microtubule detachment in gliding motility assays limits the performance of kinesin-driven molecular shuttless. Langmuir. **36**(27), 7901–7907 (2020). https://doi.org/10.1021/acs.langmuir.0c01002
11. Nitta, T., Tanahashi, A., Hirano, M., Hess, H.: Simulating molecular shuttle movements: Towards computer-aided design of nanoscale transport systems. Lab. Chip. **6**(7), 881 (2006). https://doi.org/10.1039/b601754a

12. Nitta, T., Tanahashi, A., Hirano, M.: In silico design and testing of guiding tracks for molecular shuttles powered by kinesin motors. Lab. Chip. **10**(11), 1447 (2010). https://doi.org/10.1039/b926210e
13. Ishigure, Y., Nitta, T.: Understanding the Guiding of Kinesin/Microtubule-Based Microtransporters in Microfabricated Tracks. Langmuir **30**(40), 12089–12096 (2014). https://doi.org/10.1021/la5021884